

A Method for Fast Estimation of the Rate-Limiting Step in Lithium-Ion Batteries

Miran Gaberšček

National Institute of Chemistry, Hajdrihova 19, SI-1000 Ljubljana, Slovenia

* Corresponding author: miran.gaberscek@ki.si

Received: 20-12-2013

Dedicated to the memory of Prof. Dr. Marija Kosec.

Abstract

Transport of charge in electrodes for lithium-ion batteries is complex. For accurate description one needs to use a multilevel approach which addresses processes on different scales – from the ones occurring inside active nanoparticles to those governing the transport in composite electrodes or in separators of sub-millimeter thickness. Here we attempt an approximation that allows for a fast estimation of the rate-limiting step in given electrochemical cell. Despite thoroughly simplified description of transport, the method gives surprisingly good prediction of polarisation resistance as a function of charge/discharge rate and of the electrode thickness. The method might be helpful for fast evaluation of new materials or new electrode designs in everyday laboratory testing.

Keywords: Lithium ion batteries, charge transport, electrode thickness, rate performance, electronic wiring

1. Introduction

Lithium insertion batteries rely on a mechanism whereby lithium is inserted/deinserted into/from a suitable host material.¹ This means that the lithium component needs to move (quite rapidly) within the host before it is stored at appropriate sites. As solid state diffusion of atoms (or ions coupled with electrons) at room temperature proceeds extremely slowly (chemical diffusion coefficients are down to 10^{-20} m²/s),² the active materials need to be prepared in a form of very small particles, usually on the order of 100 nm or even smaller.^{3,4} On the other hand, a huge number of such small particles (10^{12} to 10^{14} per 1 cm²) need to be deposited on metallic substrates in order to achieve useful capacities (energy densities) of practical batteries. Already a quick estimation shows that in principle there are three major transport steps (Fig. 1).

Step A represents the transport of ions and electrons from their respective reservoirs (bulk electrolyte, metallic substrate) to each individual active particle. Step B represents the insertion of electrons and ions from just the outside of particles into the particles' interior. Step C describes the transport of lithium component (coordinated movement of Li ions and electrons, also termed chemical diffusion) inside active particles.

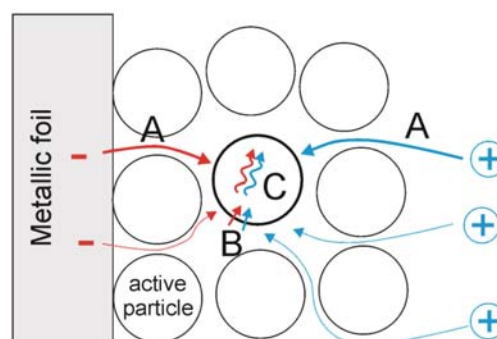


Fig. 1. Schematics of three main transport steps in an insertion battery. The circles correspond to individual active particle which are supposed to be in electronic and ionic contact to the surrounding phases. On the right there is an ionic reservoir (electrolyte in separator etc), the electrons are provided via the metallic substrate. For clarity, additives such as carbon black, binder etc are not displayed. Note that the number of active particles along the electrode thickness (several tens of micrometres) can easily exceed 1000 (which can make step A very important).

There are no obvious and simple criteria available to discern between the three possible steps. Specifically, if we prepare an insertion electrode and submit it to the usual characterization (galvanostatic testing, structural,

morphological etc. examination) one cannot say which of the three steps is determining the overall transport rate. Even more, in the literature one can find contradictory hypotheses or even “proofs” that one or the other step is more important (even for the same type of material).⁵ To some extent this is not surprising as the importance of various steps will depend on parameters such as electrode thickness (active material loading), particle size and size distribution, electrode porosity, particle conductivity, amount and distribution of conductive and non-conductive additives etc.

The lack of knowledge about the significance of transport steps certainly prevents controlled optimisation of transport for specific cases of interest. There are, of course, various tools for investigation of transport available. Most of them, however, rely on knowledge of many materials and transport parameters so investigation of a particular example can become complex and lengthy.^{6–12}

Recently, several papers^{13–15} have emerged which address the complexity of the many processes taking place inside batteries in a simplified but still in quite accurate way. The authors have succeeded to identify several macroscopic parameters, such as the generalized rate limitation factor etc., and evaluated their behaviour as a function of macroscopic electrode properties (thickness, porosity, presence of additives etc).

Here we develop a simpler (though less accurate) tool that can give rather quick insight into the main transport processes in any insertion electrode. The method requires merely two to three sets of experiments. A general approximate equation is developed that can describe the transport probed in these basic sets of experiments. The method is checked on various practical materials. The aim is to give a very general insight into the importance of two selected steps (wiring and solid state diffusion) into the behaviour of standard electrodes.

2. Experimental

2. 1. Materials Preparation

LiCoO₂ based cells were prepared using a commercial LiCoO₂ (Cathode powder SC 20, Merck, average particle size 2–3 μm). LiFePO₄/C composites were synthesized according to a citrate-precursor method described elsewhere.⁵ Briefly, an equimolar aqueous solution of LiH₂PO₄ was prepared from H₃PO₄ (Merck 1.00573) and Li₃PO₄ (Aldrich, 33,889–3). Separately, Fe(III) citrate (Aldrich, 22,897–4) was dissolved in water at 60 °C. The solutions were mixed together. After 1 h the water was removed by stirring a rotary evaporator at 60 °C under reduced pressure. The obtained xerogel was fired in argon atmosphere for 10 h at 600–700 °C. The heating rate was 10 K/min. Porous LiFePO₄ particles of typical sizes on the order of 10 micrometers were obtained. All particle surfaces were covered with a several nm thick carbon film as a

result of pyrolytic degradation of added citrate.¹⁶ The thickness was evaluated using high resolution transmission electron microscopy (HRTEM), as demonstrated in previous reference.¹⁶ The total carbon content was about 3–4 wt. %. All cathode composites were prepared from the basic active materials (either the pure LiCoO₂ or the LiFePO₄/C composite) to which carbon black (ECP 600JD) and PTFE binder (60 wt. % dispersion, Aldrich) were added to get a final weight ratio of 80:10:10 or 70:20:10. An ethanol slurry from active material, teflon and carbon black was prepared by mixing in a ball mill. Before use the ethanol was removed from the slurry.

2. 2. Electrode Preparation

The electrodes were prepared by deposition of the cathode composite onto an aluminum current collector. The surface of the latter foil was pre-ground using a sandpaper. The typical loading of electrode material was 3–7 mg/cm² of current collector. In the experiments with variable electrode thickness extra thin and thick electrodes were prepared (1–40 mg/cm²). In the case of LiCoO₂, the electrodes were pre-pressed at 5 tons for 30 seconds. Finally they were dried overnight at 110 °C and stored in a glove box.

2. 3. Electrochemical Measurements

The electrochemical characteristics were measured in a vacuum sealed cells compounded of triplex foil jacket (pouch cells). For impedance measurements three-electrode cells were prepared with metallic lithium serving both as counter and reference electrode. As the separator we used glass fiber filter paper (Whatman, Glass Microfiber Binder Free GF/A). The galvanostatic curves were recorded on two-electrode cells were constructed by using two LiCoO₂, LiFePO₄/C or TiO₂ electrodes as working and lithium as counted electrodes. The electrodes were divided by a single sheet of polymer-based separator (Celgard 2300 Microporous Membrane). The electrolyte used was a 1 M solution of LiPF₆ in ethyl carbonate/diethyl carbonate (EC:DEC = 1:1 ratio by volume, all received from Aldrich).

Electrochemical impedance spectra were recorded either with a Hewlett Packard 4284A instrument or a Solartron SI 1260 device coupled with a PAR EG&G 283 potentiostat/galvanostat. The galvanostatic characterization was performed using a VPM3 potentiostat/galvanostat. All the measurements were conducted at room temperature.

3. Model Development

3. 1. The Role of Transport Step B (Insertion/Deinsertion of Charge)

In the literature it is frequently assumed that the lithium insertion/deinsertion process (step B in Fig. 1) can

become obstructed under various conditions and that this obstruction will have a pronounced effect on the total lithium transport.^{3,17–20} In other words, these studies implicitly suppose that step B is the rate determining under certain circumstances. We show in continuation that such an assumption is reasonable when the particle size is relatively big (roughly above 1 micrometre) but gets less important, if not negligible, when the particle size is decreased to about or below 100 nm, especially if the diffusion coefficient inside the particles is low.

If the particle size is about 1 micrometre and the density is 3 g/cm³ then the specific surface area of densely packed particles is about 2 m²/g. A typical electrode loading is 1–10 mg of active material per 1 cm² of metallic substrate which then gives a total active surface of 20–200 cm². Such a surface area can be nicely probed using impedance spectroscopy because the interfacial capacity (double layer capacity) is in the range of 10⁻⁵ F/cm² × (20–200) cm² = 0.2–2 mF.⁵ This means that in impedance spectrum one will observe a medium frequency arc, such as displayed in Fig. 2a (note that here the arc was artificially emphasized by taking a smaller electrolyte concentration than usual so that the insertion resistance was significantly increased). Using a careful impedance spectroscopy approach on various systems, one can find a value of a typical normalised insertion resistance, $R_{int,0}$. For LiCoO₂ we have found a value of about 1000 Ohm per 1 cm² of active surface area, that is $R_{int,0} = 1000 \Omega\text{cm}^2$. This is a central value that can lead us to a couple of useful estimations. For example, if we prepare electrodes in which the surface area of active material will be about 1000 cm², the interfacial resistance will only be about 1 Ohm which is usually on the limit of detection in impedance spectrum. How can such an electrode be prepared? There are two obvious ways: (1) by increasing the loading per 1 cm² or (2) by decreasing the particle size. Let us check how this works with other electrode types, for example LiFePO₄. Assuming that it has a similar value for $R_{int,0}$ we realize that this material is usually used in a form of much smaller particle size but of similar electrode loading.

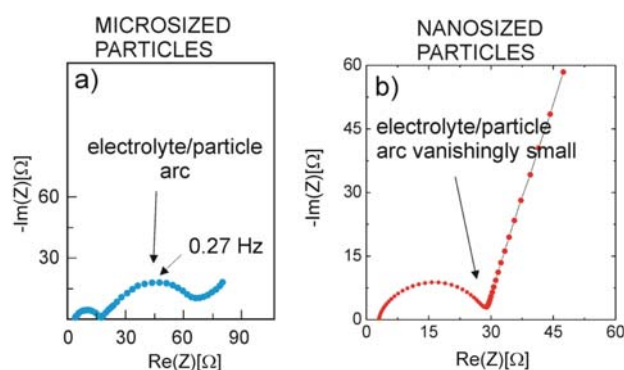


Fig. 2 Impedance response of a) a LiCoO₂ electrode (particle size between 1 and 2 micrometre and b) a LiFePO₄ electrode (particle size about 100 nm).

Specifically, we used in Fig. 2b a LiFePO₄ material with a specific surface area of 25 m²/g (particle size about 100 nm) and loading 7 mg which gives for the actual active surface area a value of 1750 cm². The actual interfacial resistance is then merely 1000/1750 Ω = 0.57 Ω. This is too small to be observed by impedance (see Fig. 2b where the medium-frequency spectrum is not observed). Namely the resolution is too low to see an arc of a size on the order of 1 Ω or lower.

The measurements and the discussion above show that in nanosized active materials the actual interfacial resistance is probably very small (due to comparably big surface area). Thus, in continuation we will neglect this contribution and focus on the other two steps, step A and C (see Fig. 1).

3. 2. The Role of Steps A and C (as Defined in Fig. 1)

In continuation we neglect step B (Fig. 1) and focus on the role of steps A and C (transport of charges from their reservoirs to the active particles and transport inside the active particles, respectively). In the corresponding impedance spectra (Fig. 2b) part of transport A is seen as the high frequency section from the origin of complex plane to the beginning of the high frequency arc (bulk electrolyte resistance) and the high frequency arc itself (resistance or electronic contact at the metal/electrode composite interface). Transport C is seen as the low-frequency line extending from ca 1 Hz to very low frequencies (usually the lowest recorded frequencies are on the order of 10⁻⁵ Hz). It needs to be said that other steps (particle-to-particle resistance, diffusion inside pores of active material etc.) might also be present but they are usually not clearly visible in the impedance spectra.⁵

If there are two important steps (such as A and C), it is frequently of interest which one represents the bigger obstacle for the transport during charge/discharge. Impedance spectroscopy can probably give some hints but it has one problem: this is a small-signal technique and is thus only able to predict the linearised regime. By contrast, the usual galvanostatic charge/discharge experiment is a large signal method, so large perturbations are involved which can make a crucial difference. If so, there appears a fundamental question: Is it possible to get a quantitative evaluation of the two transport steps (even if a rough one) from the usual galvanostatic curves? In continuation we present such a model developed explicitly for this kind of general evaluation of electrode transport.

3. 3. A Model Including Steps A and C

3. 3. 1. Basic Assumptions

It is clear from daily routine of a battery researcher that the measured battery capacity depends crucially on the rate of charge/discharge (C-rate).²¹ Here we assume

that the drop of capacity with rate is predominantly due to decreased depth of penetration of the lithium component with increasing rate – regardless of the penetration mechanism (solid state diffusion, phase boundary movement etc.). This assumption is possible because in the galvanostatic measurement there exists a cut-off voltage which stops the experiment before the lithium phase can penetrate fully into (become extracted out of) the initial phase. If so, then there should exist a quantity such as the “effective penetration depth” at given rate. This would mean that at any rate we could define an effective distance to which lithium has penetrated into (out of) every active particle. The treatment becomes especially trivial if we assume that there is a phase boundary movement and that the boundary is sharp. Then the penetration depth can be considered proportional to the charge moved, in other word proportional to the measured capacity. This is a rough approximation but at the general level of description, such as used in this paper, it may show quite good prediction capability.

3.3.2. The Calculation Procedure

First the capacity is measured as a function of charge/discharge rate (Fig. 3a). It is easier if the charge and discharge are the same and the procedure is more accurate if both processes are as symmetrical as possible. The measured capacities are then plotted as a function of current (we use the units of A/g). Then an arbitrary polynomial is selected to fit the points on this graph (Fig. 3b). In this particular case, the following polynomial gave a good fit:

$$q = q_0 - \text{Const} \times I^{0.33} \quad (1)$$

where $q_0 = 170$ mAh/g and $\text{Const} = 79.4$ (in the units of mAh/g divided by $(\text{A/g})^{0.33}$).

The fact that the fit is carried out using an arbitrary function might be disturbing but this can be understood if we know that this arbitrary function is in fact used merely

to estimate which is the fraction of the theoretical charge that is exchanged at given rate.

In the next step we extract another type of information from the galvanostatic curve – the voltage polarisation (departure from the equilibrium voltage) at given normalised current. Again, the polarisation is plotted as a function of normalised current rate (or vice versa, see Fig. 4). Now our main hypothesis (point 3.3.1) is used to determine the fitting function for current-polarisation measured points. Namely, if there is a sharp boundary being created (or if any approximation for an effective penetration depth is applicable), then one can calculate the polarisation resistance, R_p , of the probed (penetrated) part, regardless of the particle shape:

$$R_p = \frac{\xi_{chem} \rho r_0^2}{15} \left(\left(1 - \frac{q}{q_0} \right)^{-1/3} - 1 \right) \quad (2)$$

where ξ_{chem} is the general chemical resistance occurring due to coupled (chemical) diffusion of oppositely charges (such as ion and electron):²²

$$\xi_{chem} = \sigma_{chem}^{-1} = \frac{\sigma_{ion} + \sigma_{electron}}{\sigma_{ion} \sigma_{electron}} \quad (3),$$

ρ is the particle density, r_0 is its radius, σ_{ion} is the ionic and $\sigma_{electron}$ the electronic conductivity of the active particle. The chemical resistance (or its inverse, the chemical conductivity, σ_{chem}) can be related to the chemical diffusion coefficient (written for a monovalent, 1:1 stoichiometry):

$$D_{chem} = \frac{1}{\xi_{chem}} \frac{RT}{c_0 F^2} \quad (4)$$

where R is the gas constant, T is temperature, c_0 is the bulk concentration of ions/electrons and F is the Faraday's constant.

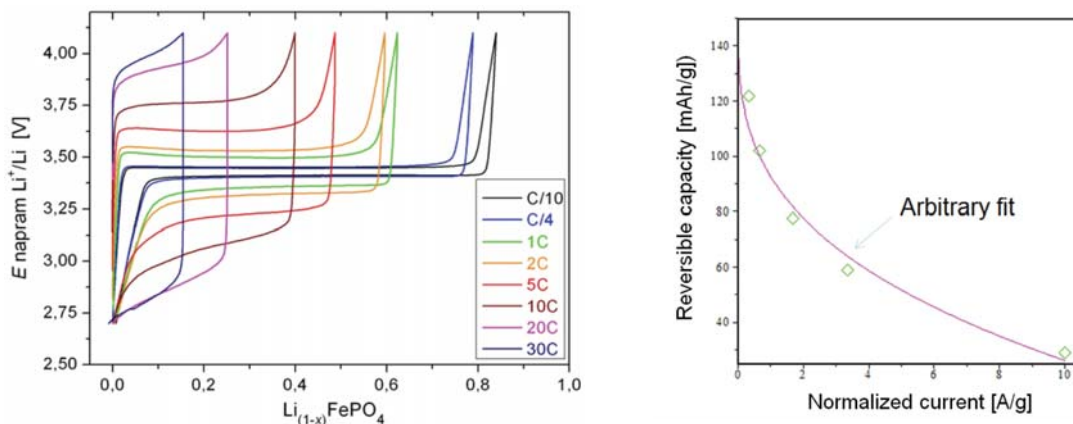


Fig. 3. A) The charge/discharge galvanostatic curves of our reference LiFePO₄ material measured at different charge/discharge rates. B) The measured capacities as a function of normalised current and a fit (solid line) using an arbitrary polynomial (see Eq. (1) and the main text).

In Fig. 4 R_p appears as the inverse of the slope of the graph.

Until now we have only considered the contribution of transport process C (transport inside active particle). We also need to add the contribution of transport A (electronic and ionic wiring). This contribution can easily be incorporated as a single resistive parameter, let us term it the wiring resistance, R_{wiring} . Finally, in general, the graph in Fig. 4 has a finite voltage value at zero current (see ref).²¹ Taking into account this finite zero-current voltage (U_0), Eq.(2) and R_{wiring} the fitting curve for Fig. 4 reads:

$$I = \frac{U_{tot} - U_0}{R_p + R_{wiring}} \quad (5)$$

where U_{tot} is the total voltage polarisation. Curves generated using Eq. 3 are completely determined with 3 parameters. There are basically also merely 3 unknowns in the materials properties, that is ξ_{chem} , U_0 and R_{wiring} . All the other quantities such as particle size or bulk concentrations, particle density etc. can be determined or estimated independently. For example, in our case the $q:q_0$ ratio appearing in Eq. (2) (and thus in Eq. 5) is determined independently from curves such as the one shown in Fig. 3. Some cross check is possible by considering the fitted value of ξ_{chem} which is correlated to chemical diffusion coefficient via Eq. (4). For LiFePO_4 typical values for ξ_{chem} are on the order of $10^9 \text{ } \Omega\text{m}$ which corresponds to a diffusion coefficient

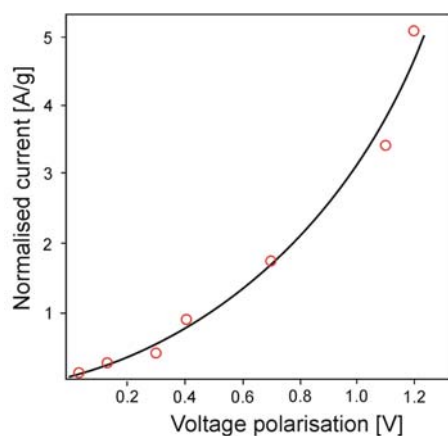


Fig. 4. Normalised current as a function of voltage polarisation. Red points are experimentally determined from galvanostatic curves shown in Fig. 3a whereas the solid line is a fit using Eq. (5). Note that only 3 free parameters were used in the fitting: ξ_{chem} , R_{wiring} and U_0 .

of 10^{-18} to $10^{-19} \text{ m}^2/\text{s}$, depending on the bulk concentration of carriers, c_0 (see Eq(4)). This, however, agrees very well with the literature data obtained by independent methods.² This reasonable value, to some extent, justifies the assumptions made in point 3.3.1.

3. 4. Further Extension of the Approach

As mentioned in the Introduction section, there is an additional parameter that can modify the number of particles per unit surface area of metallic substrate. This is the so called active material loading, that is, the mass of active material per unit surface area of substrate. Effectively, this changes the electrode thickness and thus the relative importance of transport steps A and C. This relatively simple variation (only sporadically used in the literature, e.g. in²³) may be crucial for deeper evaluation of both steps and also for optimisation of electrode thickness.

In continuation we present the results on various insertion materials. The approach can be extended to almost any insertion material.

4. Results and Discussion

We have selected data from 4 different insertion electrode materials studied previously in our laboratory: LiFePO_4 ,^{4,21,23} LiMnPO_4 ,²⁴ TiO_2 ²⁵ and LiCoO_2 .⁵ Electrodes with different masses were compared, from very thin (<1mg of mass per 1cm^2 of collector) to very thick (<70 mg/cm^2) ones. Compositional and morphological data (particle size, amount and type of additives, electrode thickness, pressure on electrode etc) were compared to impedance (of dry and wet electrodes) and electrochemical data.

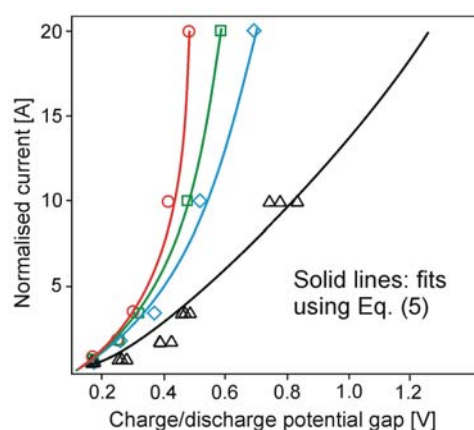


Fig. 5. Normalised current as a function of voltage polarisation for 4 different masses (loadings) of LiFePO_4 electrodes. Only the red curve (the lowest mass) was fitted, the other solid curves were automatically predicted from Eq. (5). Loadings (in mg of active material per 1 cm^2 of aluminium collector): red circles = 1.1; green squares = 2.5; blue diamonds = 4.5; black triangles = 9.3 (three different samples were measured in this case).

Note that when a series of electrodes of different masses is used, the system becomes additionally constrained. This means less freedom when the fitting procedure is applied. For example in Fig. 5 we show a set of 4 curves corresponding to different electrode masses, the bigger

the mass the bigger is the polarisation. However, it needs to be stressed that one curve alone is needed to determine all of the parameters – the other 3 are determined automatically, there are no further free parameters left.

The prediction of the three curves' shapes and values is surprisingly good (which indirectly additionally justifies the model assumptions).

The results of Fig. 5 can alternatively be represented in a graph where the total resistance $R_p + R_{wiring}$ is plotted as a function of electrode mass (Fig. 6). Two extreme results are shown: a) for the case of good wiring ($R_{wiring} \ll R_p$) and b) for the case of comparable values of both resistances ($R_{wiring} \approx R_p$). In the former case (TiO_2), there is no minimum which means that wiring was good in all cases, so the electrode thickness (loading of active mass) could be further increased without compromising the rate performance. In the second case (LiCoO_2), however, the wiring began to become essential when the loading reached values around 10 mg/cm^2 which is demonstrated as a minimum in the curves. It is worth noting that the position of minimum depends to some extent on the current rate (the minimum is shifted to lower loading as the rate increases).

The importance of wiring in thicker electrodes has been widely discussed in previous works.^{26–30} The present results entirely agree with those earlier reports, although the present treatment is considerably simplified.

5. Conclusions

Carrying out and comparing the results on various systems mentioned, the following conclusions can be made:

1. When the particle size decreases below about 200–300 nm, there remain only two main transport steps:
 - a) the transport of charges from their reservoirs (collector, electrolyte) to the active particles (step A, or “wiring step”)

- b) the transport inside the active particles (step C or “solid state transport step”)

2. The wiring step starts to prevail at electrode loadings of $10\text{--}20 \text{ mg/cm}^2$. An essential part (usually more than 50%) of wiring is the transport of electrons from the current collector to the active mass. The total wiring resistance amounts between ca 5 and 20Ω per 1 cm^2 of current collector. This means that the maximum currents that can be sustained when wiring is the limiting step are on the order of $0.1\text{--}0.4 \text{ A}$ (or $10\text{--}40 \text{ A/g}$) in 10 mg electrodes. Practical results published in the literature confirm this estimation. Even more, due to wiring it is unreasonable to expect much higher current values. So when bigger currents are measured one needs to check the results with respect to possible artefacts (e.g. wrong estimation of mass etc.).

3. In most materials the electronic conductivity seems to be better than the ionic (estimated from the value of ξ_{chem} in Eq. 3 and comparing it to the so called “dry measurements” where merely the electronic component or resistance is measured). This means that optimization of electrode mass needs to be focused on providing sufficient ionic conductivity/supply – such as maintenance of porosity etc. Of course the role of electronic conductivity in terms of contact resistance should not be neglected – in practical cases this could be one of major origins for poor electrode performance.

4. Decrease of particle size is probably the only really effective way to improve the rate performance and also safety at higher powers (prevention of excessive heat generation). However, any agglomeration needs to be prevented in order to exploit the true benefits of decreased particle size (only then equations (3–5) are valid in the form presented).

5. The role of surface decorations^{3,17–20,25} is not necessarily to decrease the insertion resistance. The latter is already very small in »normal« nanosized materials. The role could be either prevention of agglomeration or improvement of wetting of particles with electrolyte.

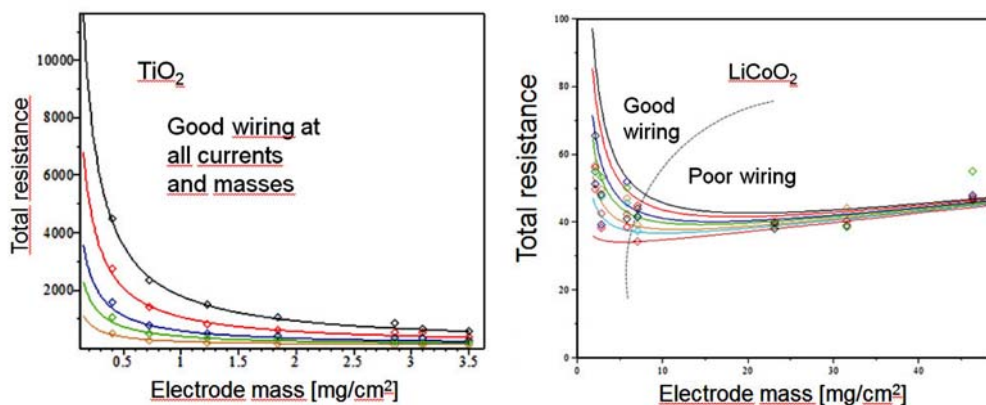


Fig. 6. Total resistance ($R_p + R_{wiring}$ in Ohms) as a function of electrode mass for TiO_2 and LiCoO_2 electrodes. Various C-rates are represented, the top curves correspond to smallest rate, the bottom to the highest rate. Note again the excellent prediction (only one rate is fitted, the others are determined automatically). Note a minimum on the right and its absence on the left. More comments are given in the main text.

In the end, the reader should be cautioned that our treatment is only valid if the widely accepted standard conditions are met in preparation and measurement of electrodes. Namely, there are occasional reports where exceptional results are reported such as very fast charge-discharge rates^{31–33} that are difficult to be interpreted within those standard limitations. It is difficult to imagine that charging would be faster than is the time needed to insert the lithium into all of the active particles and this is rigidly determined by transport in solid state – whatever the exact mechanism. Faster times can only be achieved if, for example: a) we are satisfied with only partially charged electrode, b) we have additional material that can be charged faster (e.g. in terms of supercapacitance etc), c) the structure of active material deviates from the usual one – so as to facilitate the solid state transport, d) the known transport data (diffusion coefficient, conductivities) are wrongly estimated (or the mechanism is not entirely understood. It is difficult to evaluate which of these factors plays the important role in such outstanding results (probably several of them).

6. Acknowledgments

The autor thanks Dr. Jože Moškon for carrying out the experimental part. Financial support from the Slovenian Research Agency is fully acknowledged. Part of the work was carried out within the FP7 project “Euroliion”.

7. References

1. J.-M. Tarascon, M. Armand, *Nature* **2001**, *414*, 359.
2. P. P. Prosini, M. Lisi, D. Zane, M. Pasquali, *Solid State Ionics* **2002**, *148*, 45–51.
3. B. Kang, G. Ceder, *Nature* **2009**, *458*, 190–193.
4. M. Gaberscek, R. Dominko, J. Jamnik, *Electrochem. Commun.* **2007**, *9*, 2778.
5. Atebamba, Moškon, Pejovnik, Gaberšček, *J. Electrochem. Soc.* **2010**, *157*, A1218–A1228.
6. D. Dees, E. Gunen, D. Abraham, A. Jansen, J. Prakash, *J. Electrochem. Soc.* **2005**, *152*, A1409.
7. J. Newman, K. E. Thomas, H. Hafezi, D. R. Wheeler, *J. Power Sources* **2003**, *119*, 838.
8. V. Srinivasan, J. Newman, *J. Electrochem. Soc.* **2004**, *151*, A1517.
9. D. E. Stephenson, E. M. Hartman, J. N. Harb, D. R. Wheeler, *J. Electrochem. Soc.* **2007**, *154*, A1146.
10. S. Brown, N. Mellgren, M. Vynnycky, Göran Lindbergh, *J. Electrochem. Soc.* **2008**, *155*, A320.
11. G. K. Singh, G. Ceder, M. Z. Bazant, *Electrochim. Acta* **2008**, *53*, 7599–7613.
12. T. R. Ferguson, M. Z. Bazant, *J. Electrochem. Soc.* **2012**, *159*, A1967–A1985.
13. C. Fongy, A. C. Gaillot, S. Jouanneau, D. Guyomard, B. Lestriez, *J. Electrochem. Soc.* **2010**, *157*, A885.
14. C. Fongy, S. Jouanneau, D. Guyomard, J. C. Badot, B. Lestriez, *J. Electrochem. Soc.* **2010**, *157*, A1347.
15. C. Fongy, S. Jouanneau, D. Guyomard, B. Lestriez, *J. Power Sources* **2011**, *196*, 8494.
16. R. Dominko, M. Bele, J.-M. Goupil, M. Gaberscek, D. Hanzel, I. Arcon, J. Jamnik, *Chem. Mater.* **2007**, *19*, 2960–2969.
17. Y.-K. Sun, S.-W. Cho, S.-T. Myung, K. Amine, Jai Prakash, *Electrochim. Acta* **2007**, *53*, 1013.
18. D. Li, Y. Kato, K. Kobayakawa, H. Noguchi, Y. Sato, *J. Power Sources* **2006**, *160*, 1342.
19. M. M. Thackeray, C. S. Johnson, J.-S. Kim, K. C. Lauzze, J. T. Vaughney, N. Dietz, D. Abraham, S. A. Hackney, W. Zeltner, M. A. Anderson, *Electrochem. Commun.* **2003**, *5*, 752.
20. D. Aurbach, B. Markovsky, A. Rodkin, E. Levi, Y.S. Cohen, H.-J. Kim, M. Schmidt, *Electrochim. Acta* **2002**, *47*, 4291.
21. W. Dreyer, J. Jamnik, C. Gohlke, R. Huth, J. Moskon, M. Gaberscek, *Nat. Mater.* **2010**, *9*, 448.
22. M. Gaberscek, J. Jamnik, *Solid State Ionics* **2006**, *177*, 2647.
23. M. Gaberscek, M. Kuzma, J. Jamnik, *Phys. Chem. Chem. Phys.* **2007**, *9*, 1815.
24. M. Pivko, M. Bele, E. Tchernychova, N. Zabukovec Logar, R. Dominko, M. Gaberscek, *Chem. Mater.* **2012**, *24*, 1041–1047.
25. J. Jamnik, R. Dominko, B. Erjavec, M. Remskar, A. Pintar, M. Gaberscek, *Adv. Mater.* **2009**, *21*, 2715.
26. D. Y. W. Yu, K. Donoue, T. Inoue, M. Fujimoto, S. Fujitani, *J. Electrochem. Soc.* **2006**, *153*, A835.
27. P. A. Johns, M. R. Roberts, Y. Wakizaka, J. H. Sanders, J. R. Owen, *Electrochem. Commun.* **2009**, *11*, 2089.
28. N. Böckenfeld, T. Placke, M. Winter, S. Passerini, A. Balducci, *Electrochim. Acta* **2012**, *76*, 130.
29. S. Yu, S. Kim, T. Y. Kim, J. H. Nam, W. I. Cho, *J. Appl. Electrochem.* **2013**, *43*, 253.
30. J. Liu, M. Kunz, K. Chen, N. Tamura, T. J. Richardson, *J. Phys. Chem. Lett.* **2010**, *1*, 2120.
31. J. Come, P.-L. Taberna, S. Hamelet, C. Masquelier, P. Simon, *J. Electrochem. Soc.* **2011**, *158*, A1090.
32. H. Munakata, B. Takemura, T. Saito, K. Kanamura, *J. Power Sources* **2012**, *217*, 444.
33. S.-L. Wu, W. Zhang, X. Song, A. K. Shukla, G. Liu, V. Battaglia, V. Srinivasan, *J. Electrochem. Soc.* **2012**, *159*, A438.

Povzetek

Transport naboja v elektrodah za litij-ionske baterije je zapleten. Če ga želimo natančneje opisati, se moramo zateči k večnivojskim metodam. Te hkrati obravnavajo procese na različnih skalah – od takšnih, ki se odvijajo znotraj aktivnih nanodelcev do tistih, ki potekajo v kompozitni elektrodi ali separatorju, ki sta submilimetrskih dimenzij. V prispevku uvajamo poenostavljeno metodo, ki omogoča hitro ugotavljanje najpočasnejšega koraka in s tem hitrost celokupnega transporta v izbrani baterijski celici. Čeprav je metoda enostavna, daje presenetljivo dobre napovedi glede polarizacijske upornosti kot funkcije hitrosti praznjenja/polnjenja baterije oziroma kot funkcije debeline elektrode. Metoda je potencialno uporabna za hitro evalvacijo lastnosti novih materialov ali novih elektrodnih dizajnov pri vsakdanjem laboratorijskem testiranju baterij in podobnih celic.